Ferromagnetic interactions in nanostructured systems with two different Curie temperatures

I. Navarro and M. Ortuño
Departamento de Física, Universidad de Murcia, 30.071 Murcia, Spain

A. Hernando
Instituto de Magnetismo Aplicado, Universidad Complutense, P.O. Box 155 Las Rozas, Madrid 28230, Spain
(Received 12 July 1995; revised manuscript received 12 January 1996)

We study the exchange interactions between ferromagnetic grains dispersed in a paramagnetic amorphous matrix. This interaction becomes very important for high-density packing of the grains and also when the amorphous matrix is near its Curie temperature. We obtain analytical results based on a mean-field approximation and also perform a Monte Carlo simulation. We use both procedures to estimate the ordering temperature as a function of the effective intergrain separation. The theoretical predictions are compared with experimental results for the $Fe_{77}B_{18}Nb_4Cu$ nanocrystalline alloy.

I. INTRODUCTION

Magnetic nanocrystalline materials are heterogeneous systems composed of different magnetic and structural phases. We are mainly interested in magnetic materials consisting in nanocrystallites randomly nucleated in an amorphous magnetic matrix. A good example are Fe-rich nanocrystals.[1] They present outstanding technical properties and constitute some of the most promising magnetic materials.

These materials show excellent soft magnetic properties, which arise from the fact that the nanocrystallites are strongly exchange coupled via the amorphous interphase region. This coupling leads to an averaging out of the magnetic anisotropy of the individual crystalline grains.[2] Over the past few years, many groups have carried out experimental studies of soft nanocrystals of differing compositions in an attempt to characterize and understand their magnetic and structural properties.[3–6]

In this paper, we are particurlarly interested in understanding the following two recent experimental results.

(i) The Curie temperature of the matrix, T_C^a, is smaller than the Curie temperature of the α-Fe nanocrystalline grains, and, at sufficiently high tempertures, the system behaves as an assembly of isolated single-domain particles. However, the thermal dependence of the coercive force[7] indicates that the α-Fe grains strongly interact in a wide range of temperatures above T_C^a. Coupling is observed even 100 °C above T_C^a.[8]

(ii) Recently, it has been observed that the Curie temperature of the intergranular amorphous region is greatly enhanced with respect to that of amorphous ribbons of the same composition, this enhancement reaching a value of 125 °C.[9]

These experimental results have led us to study the intergrain exchange interactions mediated by the amorphous matrix. We show that the predicted ordering temperature of the grains is the right order of magnitude to explain the experimental results on the nanocrystalline $Fe_{77}B_{18}Nb_4Cu$ alloy.[10] We use two different methods, an analytical mean-field approach and a direct numerical simulation, to obtain the effective intergrain exchange. In both approaches, we assume a single exchange interaction J between atoms of the amorphous matrix. The amorphous structure is simulated by a simple cubic lattice. We consider only nearest neighbor interactions, and calculate J from the transition temperature of the amorphous matrix. The presence of nanocrystalline ferromagnetic grains is modeled by ferromagnetic boundaries where the matrix spin are forced to be fully aligned.

II. MEAN-FIELD APPROACH

In the mean-field approximation, we assume that the atomic magnetic moment at site r is proportional to the sum of the magnetic moments of its nearest neighbor (NN) atoms:

$$m(r)=\frac{\chi_p\alpha}{z}\sum_{\mathrm{NN}} m(r')=\frac{T_C}{zT}\sum_{\mathrm{NN}} m(r'), \tag{1}$$

where χ_p is the paramagnetic susceptibilty of the material, in the absence of interactions between atoms, α is the proportionality constant of the molecular-field approximation, and z is the coordination number. We restrict the analysis to a simple cubic lattice for which $z=6$. We assumed that the paramagnetic susceptibility in the absence of interactions follows the Curies' law $\chi_p \propto 1/T$ and so the final susceptibility (considering interactions in the mean-field approximation) follows the Curie-Weiss law $\chi=\chi_p/(1-T_C/T)$, where T_C is the Curie temperature.

Above the Curie temperature, if there is no applied magnetic field and no ferromagnetic boundary, the self-consistent solution of Eq. (1) is $m(r)=0$ for all r. The presence of a ferromagnetic boundary induces a finite magnetization near the boundary even above T_C, and it is this magnetization that we wish to calculate.

A. Single-plane problem

Let us first consider a Y-Z plane boundary where the atomic magnetic moments are equal to 1 (see Fig. 1). By symmetry, the magnetic moment m_i of an atom in the ith layer, with respect to the surface, only depends on the dis-

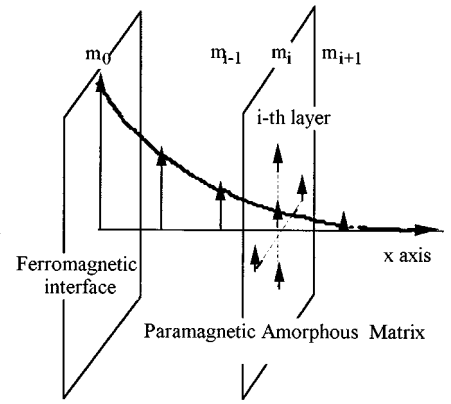

FIG. 1. Simplified scheme of the single-plane problem geometry.

tance to the surface. Equation (1), therefore, leads to the following recurrence relation between magnetic moments of adjacent layers:

$$Am_i = m_{i-1} + m_{i+1}, \tag{2}$$

where $A = (zT/T_C) - z + 2$. This expression is subjected to the boundary condition $m_0 = 1$. Its solution, which must tend to zero when we move away from the ferromagnetic surface, is of the form $m_i = s m_{i-1}$, where s is a constant between 0 and 1, to ensure convergence. Substituting this expression in Eq. (2) and considering $z = 6$, we find that s is given by

$$s = (3t-2) - \sqrt{(3t-2)^2 - 1}, \tag{3}$$

where t is the reduced temperature, defined as the ratio $t = T/T_C$.

The magnetic moment of an atom located at the ith layer is then equal to

$$m_i = s^i. \tag{4}$$

Expression (4) presents an exponential decrease with the distance to the ferromagnetic interface and its analogous continuous form is

$$m(x) = \frac{e^{-x/\lambda}}{a^3}, \tag{5}$$

where x is the distance to the interface, a is the separation between nearest neighbor atoms, and $\lambda = -a/\ln(s)$ is the penetration length of the interaction, which only depends on the reduced temperature t. This continuous approximation is useful for the calculation of the magnetization in the presence of spherical ferromagnetic boundaries, and is well justified when the magnetization does not decrease too drastically, which is precisely the regime where the exchange interaction is important. It is to be noted that a similar phenomenological dependence was introduced by Hernando *et al.*[11] to account for the exchange coupling between grains above T_C^a.

The total magnetic exchange energy per unit area is equal to

$$E^{(1p)} = -\frac{J}{a^2}\sum_{i=1}^{\infty}(2m_i^2 + m_i m_{i-1}) = -\frac{J}{a^2}\frac{2s^2+s}{1-s^2}. \tag{6}$$

The corresponding quantity in the continuous formulation is given by

$$E^{(1p)} = -3Ja^3\int_{a'}^{\infty} m(x)^2 dx = -\frac{3J\lambda}{2a^3}e^{-2a'/\lambda}. \tag{7}$$

The continuous and discrete procedures give very similar values for the exchange energy, in the temperature range of interest $(1.1 < t < 3)$, if $a' = 0.36a$ is chosen as the lower integration limit.

B. Two-plane problem

We study the interaction energy between ferromagnetic plane surfaces through the magnetization induced in the paramagnetic matrix between them. We consider that the magnetizations of the two boundaries lie in the plane surface, either parallel or antiparallel between them. The results of this problem are useful for understanding the interaction between ferromagnetic grains in nanocrystalline materials, and have an intrinsic interest for the explanation of experimental results about multilayer systems.[12]

Let us assume that our paramagnetic system is now in contact with two ferromagnetic parallel plane surfaces, at $x = 0$ and $x = \Lambda$ (interphase thickness). The magnetic moment of each atom is the sum of two contributions of the form given by Eq. (5), due to the two boundary conditions of the system. The sign of these components depends on whether the surface magnetization is parallel or antiparallel. The total exchange energy, per unit area, of the intephase medium is then equal to

$$E^{(2p)} = -\frac{3J\lambda}{a^3}(e^{-2a'/\lambda} - e^{-2(\Lambda - a')/\lambda}) \mp \frac{6J\Lambda}{a^3}e^{-\Lambda/\lambda}. \tag{8}$$

The $-(+)$ sign corresponds to parallel (antiparallel) magnetization of the boundary surfaces. The first term in this equation is twice the energy of one isolated ferromagnetic interface, cut at $x = \Lambda$. The second term is due to the interaction between the magnetic moments induced by different planes, and represents the effective coupling between the two ferromagnetic planes through the paramagnetic interphase. This coupling has an exponential dependence on the ratio between the effective intergrain separation Λ and the penetration length λ, and is propotional to the number of atoms between the planes.

C. Two-sphere problem

We can now estimate the effective exchange coupling between two spherical ferromagnetic grains through the paramagnetic medium between them. We assume that this coupling is equal to the product of the exchange coupling per surface unit for the two planes and an effective surface of the grains, which takes into account the area of each grain that is closest to another.

Let us call Λ the minimum separation between grains. Our effective surface is equal to the area of a grain located at a distance smaller than $\Lambda + \lambda$ from the other grain, as is shown in Fig. 2. We assume that only atoms separated by

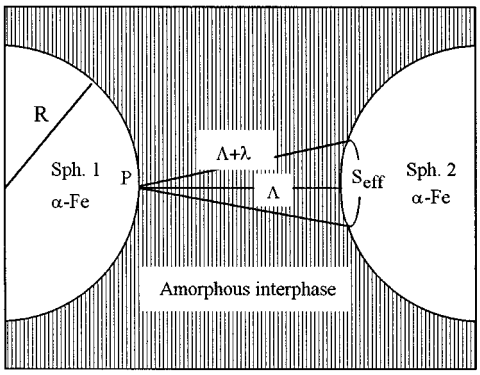

FIG. 2. Effective surface of a ferromagnetic sphere and system geometry of the Ising simulation.

distances between Λ and $\Lambda+\lambda$ interact appreciably. The number of atoms in the effective surface ranges between 50 and 200 for a typical crystalline volume fraction and in the temperature range of interest.

The effective coupling between grains is then equal to

$$J_{\text{eff}}^{(\text{sph})} = -\frac{12J\Lambda R^2}{a^3}\arcsin\left(\frac{\sqrt{\lambda^2+2\lambda\Lambda}}{R}\right)e^{-\Lambda/\lambda}, \qquad (9)$$

where R is the sphere radius. This exchange interaction energy is the product of the number of atoms between the effective surfaces and an exponential factor. This number of atoms is fairly independent of temperature and of the order of 500. The exponential factor is very sensitive to the effective intergrain separation Λ and to the reduced temperature t.

III. NUMERICAL SIMULATION

We have also calculated the effective coupling between ferromagnetic nanocrystals embedded in an amorphous paramagnetic matrix by direct numerical simulation. We assume an Ising system in a simple cubic lattice subjected to different boundary conditions, corresponding to the different possible magnetizations of the nanocrystals. We use a Metropolis algorithm to thermalize the samples and to generate a succession of independent configurations with a thermal distribution. The algorithm performs 300 Monte Carlo sweeps for thermalization and 100 sweeps between successive measurable configurations. For each configuration we calculate the exchange interaction energy, which only depends on the relative orientation between magnetic moments of nearest neighbor atoms. The total exchange energy at each temperature is averaged over a large set of independent configurations, whose number ranges between 500 and 1000.

The system consists of a cylinder of length $2R+\Lambda$ containing two semispherical Fe grains with their corresponding centers lying on the two bases of the cylinder, as shown in Fig. 2. We consider a sphere radius (R) of 10 lattice spacings, which corresponds to 3.5 nm, and a separation between spheres of 3, 6, and 12 lattice spacings, corresponding to 1, 2, and 4 nm. The grains have fixed magnetizations, perpendicular to the axis of the cylinder, whose relative orientation can be either parallel or antiparallel. We apply free boundary conditions at the lateral cylinder surface and periodic (antiperiodic) at the bases in a parallel (antiparallel) configuration. The effective exchange coupling is equal to half the total energy difference between the configurations corresponding to parallel and antiparallel boundary conditions.

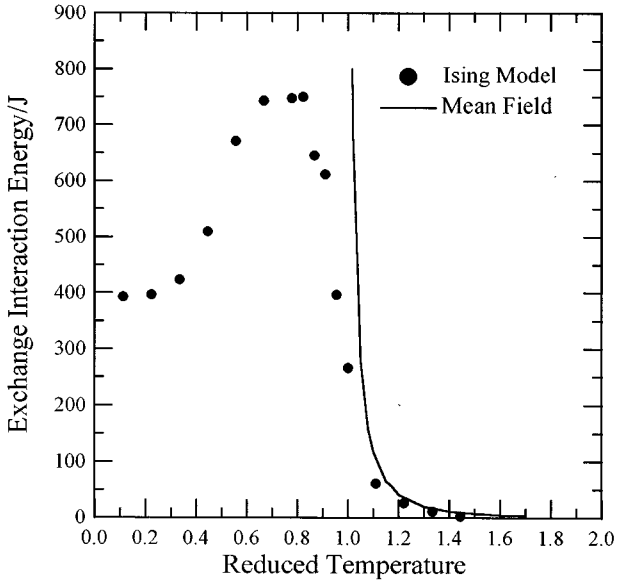

FIG. 3. Theoretical effective exchange coupling versus the reduced temperature for ferromagnetic spheres of radius 3.5 nm and $\Lambda=1$ nm, obtained by a mean-field approach (solid line) and Monte Carlo simulation (solid points).

In Fig. 3 we show the effective coupling between spheres as a function of the reduced temperature for a separation Λ of 1 nm, obtained by the mean-field aproach (solid line) and Monte Carlo simulation (solid points). We choose the value $T_C=4.5J/K_B$ for the critical temperature of the three-dimensional Ising model,[13] where K_B is the Boltzmann constant. The mean-field analytical results and the numerical simulations agree fairly well in the region of interest, i.e., for temperatures above the critical.

IV. CRITICAL TEMPERATURE

The exchange interaction studied will couple the ferromagnetic grains at temperatures higher than the Curie temperature of the amorphous matrix and will also result in an overall magnetization of the amorphous matrix when the penetration length is in the order of the typical intergrain spacing.

Thus some critical behavior associated with this exchange interaction is to be expected at a temperature T^* proportional to the effective coupling between nearest neighbor grains:

$$J_{\text{eff}} = \gamma T^*. \qquad (10)$$

The constant of proportionality γ must be similar to that relating the Curie temperature and the exchange interaction of the amorphous matrix. We assume that both constants are the same. This is justified by the fact that both the grains and the atoms of the amorphous matrix are randomly distributed in an effectively close-packed structure. In any case, the final results are very insensitive to this parameter as can be seen in the inset of Fig. 4: A change in the slope of the straight line produces almost no modification in t^*.

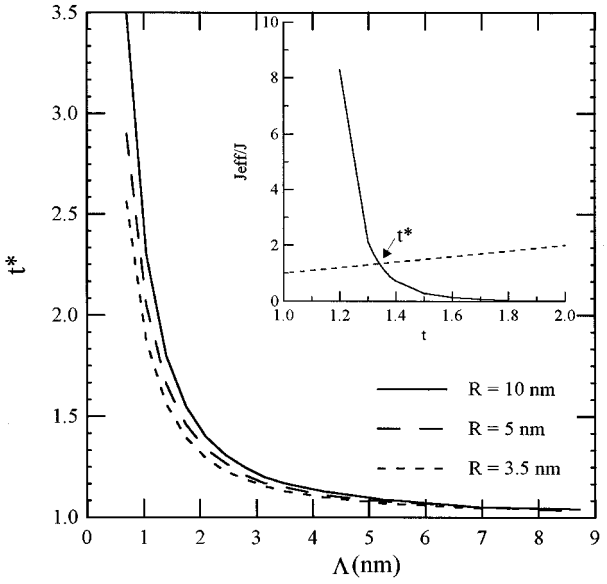

FIG. 4. Dependence of the theoretical critical temperature, in reduced units, on the effective intergrain separation for ferromagnetic spheres with a radius of 10 nm (solid line), 5 nm (long dashed line), and 3.5 nm (short dashed line). The inset shows an example of the procedure followed to calculate the critical temperature.

This critical temperature can be obtained from the intersection point of the curve $J_{\rm eff}/J$ [from Eq. (9)] and the straight line $J_{\rm eff}/J=t$, when both are plotted as a function of the reduced temperature t. An example of this procedure is shown in the inset of Fig. 4. To obtain the critical temperature from the numerical simulations, we fit the effective couplings by an exponential function of temperature and calculate its intersection point with the $J_{\rm eff}/J=t$ line. The small values of the effective couplings result in large errors in the fitting curve, although the final error bars in the critical temperatures are relatively small.

Figure 4 shows the calculated critical temperature, in reduced units, for the mean-field approach as a function of the effective distance between nearest neighbor grains, for spheres of 10 nm (solid line), 5 nm (long dashed line), and 3.5 nm (short dashed line) radius. We note that the results do not depend very much on the radius of the spheres. For this reason we performed our numerical simulations with the smallest realistic radius, to minimize computational effort.

In Fig. 5 we compare the theoretical critical temperatures obtained by the two procedures we used. The solid line corresponds to the mean-field results and the solid points to the numerical simulation. Both results are relatively similar, although the numerical simulation predicts smaller critical temperatures for small grain separations.

V. DISCUSSION

As we can see from Fig. 4, the exchange coupling between Fe grains through the paramagnetic interphase strongly depends on effective intergrain separation and can be effective at temperatures well above the interphase Curie temperature.

Magnetic interactions between ferromagnetic grains through a paramagnetic medium have been observed by

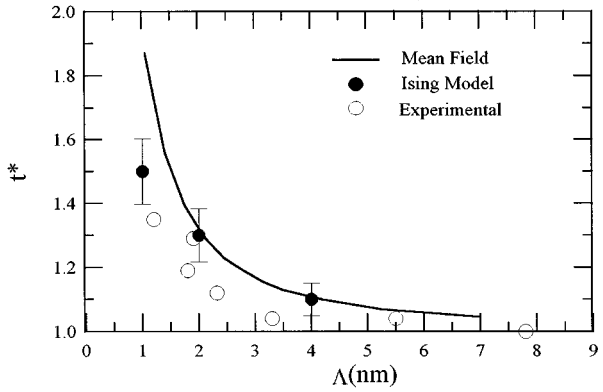

FIG. 5. Enhancement of the experimental temperature of the coercive force maximum versus the amorphous interphase Curie temperature in the $Fe_{77}B_{18}Nb_4Cu$ nanocrystalline alloy (open points) and theoretical critical temperatures, obtained by a mean-field approach (solid line) and Ising simulation (solid points), plotted as a function of the effective intergrain separation.

measuring the thermal dependence of the coercive force, in Fe-rich soft nanocrystals, which present two Curie temperatures.[8,10] At room temperature, the soft magnetic behavior is mainly due to the exchange coupling between Fe grains through the amorphous ferromagnetic medium. The gradual hardening observed when temperature increases is a consequence of the decrease in exchange coupling between Fe grains that takes place simultaneously with the loss of the amorphous interphase magnetic moment. The coercive force reaches a maximun value at a temperature (T_p). At temperatures above this maximum the coercive force decreases as a consequence of the decrease in the magnetocrystalline anisotropy of the Fe grains. The coercive force maximum occurs at temperatures close to the Curie temperature of the amorphous interphase for a small crystalline volume fraction, but at temperatures well above T_C^a for larger crystalline fraction. For a $Fe_{77}B_{18}Nb_4Cu$ nanocrystalline alloy with 40% of Fe crystallized (Λ about 1 nm), the temperature peak occurs 100 °C above T_C^a.[10]

According to the previous discussion, we take the temperature of the coercive force maximun as the critical experimental temperature to be compared with our theoretical prediction for the onset of an alignment of the grains magnetic moments. For temperatures above (T_p), the decrease of the coercive force points out that magnetic intergrain interactions become sufficiently small to be cancelled by thermal energies. The ratio between the temperature of the coercive force maximum and the Curie temperature of the amorphous material, T_p/T_C^a, plays the role of the reduced experimental critical temperature. In Fig. 5 we compare our theoretical critical temperatures with the experimental results for the $Fe_{77}B_{18}Nb_4Cu$ nanocrystalline alloy, as a function of the effective intergrain separation. We calculate the effective intergrain separation from the experimental crystalline volume fraction v and the average grain size d obtained by x-ray diffraction and Mössbauer spectroscopy techniques. Assuming a spherical shape for the grains and a single cubic distribution geometry, Λ is implicitly given by

$$v = \frac{\pi d^3}{6(d+\Lambda)^3}. \quad (11)$$

As shown in Fig. 5, the interaction mechanism proposed can explain the magnitude of the critical temperature enhancement observed and its dependence on the effective intergrain separation.

VI. CONCLUSION

The induction of magnetization by a ferromagnetic interface in a medium above its Curie temperature was calculated on the basis of a mean-molecular-field approximation and by Monte Carlo simulation. It was found that ferromagnetic spheres embedded in a paramagnetic medium are exchange coupled via the induced magnetization at the interphase. The analytically calculated exchange interaction energy is the product of the number of atoms between the effective surfaces and an exponential factor, which depends on the ratio between the effective intergrain separation and the interaction penetration length. In Fe-rich nanocrystalline materials, the small grain size and the high-density packing result in effective intergrain separation of a few nanometers. Under these conditions, the calculated exchange interaction energy must be relevant, even at temperatures well above the Curie temperature of the amorphous matrix.

A theoretical critical temperature proportional to the effective coupling between nearest neighbor grains was estimated and compared with the experimental critical temperatures. It was found that the interaction mechanism proposed can explain the temperature values corresponding to the maximum coercive force in a $Fe_{77}B_{18}Nb_4Cu$ nanocrystalline alloy.

ACKNOWLEDGMENTS

We acknowledge the financial support of the Spanish DGICYT, Project No. PB93-1125, and the CICYT, Project No. MAT95-1045-C02-02.

[1] Y. Yoshizawa, S. Oguma, and K. Yamauchi, J. Appl. Phys. **64**, 6044 (1988).
[2] R. Alben, J.J. Becker, and M.C. Chi, J. Appl. Phys. **49**, 1653 (1978).
[3] G. Herzer, IEEE. Trans. Magn. **MAG-26**, 1397 (1990).
[4] E. Pulido, I. Navarro, and A. Hernando, IEEE. Trans. Magn. **MAG-28**, 2424 (1992).
[5] T. Reininger, B. Hofmann, and H. Kromüller, J. Magn. Mater. **111**, 220 (1992).
[6] K. Suziki, A. Makino, N. Kataoka, and T. Masumoto, Mater. Trans. JIM **33-1**, 93 (1991).
[7] A. Slawska-Waniewska, M. Kuzminski, M. Gutowski, and H.L. Lachowicz, IEEE. Trans. Magn. **MAG-29**, 2628 (1993).
[8] A. Hernando and T. Kullik, Phys. Rev. B **49**, 7064 (1994).
[9] A. Hernando, I. Navarro, and P. Gorría, Phys. Rev. B **51**, 3281 (1995).
[10] I. Navarro, PhD. thesis, Universidad Complutense, Madrid, 1994.
[11] A. Hernando, M. Vazquez, T. Kullik, and C. Prados, Phys. Rev. B, **51**, 3581 (1995).
[12] A. Hernando, I. Navarro, C. Prados, D. García, M. Vazquez, and J. Alonso, Phys. Rev. B **53**, 8223 (1996).
[13] A.M. Ferrenberg and D. P. Landau, Phys. Rev. B **33**, 7841 (1986).